Photoconduction in Annealed and Chemically Treated CdSe/ZnS Inorganic Nanocrystal Films

Venda J. Porter,[†] Scott Geyer,[†] Jonathan E. Halpert,[†] Marc A. Kastner,[‡] and Moungi G. Bawendi*[,†]

Department of Chemistry and Department of Physics, Massachusetts Institute of Technology, 77 Massachusetts Avenue, Cambridge, Massachusetts 02139

Received: October 19, 2007

We present a study of photoconductivity in close-packed films of CdSe/ZnS core/shell nanocrystals, from which the majority of the organic ligands are removed. The ZnS inorganic shells separate the CdSe cores, and passivate the surface of the CdSe nanocrystals, slowing the nonradiative exciton decay rate. These films retain the size-dependent quantum-confined electronic properties of the nanocrystals, including the tunability of their band gap. We demonstrate that replacing the organic ligands, which form the tunnel barrier between nanocrystals in films of CdSe nanocrystals, with the inorganic ZnS shell results in photoconduction with near unity internal quantum efficiency at room temperature.

1. Introduction

Optoelectronic devices such as photodetectors,[1,2] lasers,[3] and solar cells[4−7] that incorporate thin films of semiconductor nanocrystals (NCs) are of increasing interest because of the flexible chemical processibility of the nanocrystals and the tunability of their effective band gap. The flexible, solution processibility of the NCs is made possible by the organic ligands that cap the NCs; however, these ligands are electrically insulating and reduce the conductivity of NC films significantly.[8,9] Methods must be developed to enhance their electrical conductivity in order to make efficient optoelectronic devices from NC films. In addition, techniques to modify the conductivity in NC films may allow the study of fundamental charge transport in these solids by tuning site energies and internanocrystal electronic coupling.

In recent years, a number of methods have been developed to increase both the dark- and photoconductivity of NC films. Thermal annealing has been employed to reduce interparticle spacing and to modify the chemical nature of the capping ligand.[10,11] Postdeposition cap exchange has also been used to decrease NC spacing by replacing the bulky trioctylphosphine or oleic acid ligands, which cap the NCs after synthesis, with smaller ligands.[12−14] In addition, the conductivity has been enhanced through chemical doping of the NCs, either with an electrochemical cell[15,16] or by cap exchange with a reducing agent such as hydrazine[17] or sodium biphenyl.[18,19] Because of the resulting enhanced dark and photocurrents, a clearer picture of the physics of charge transport in NC films has emerged. For example, variable range hopping has been observed in doped CdSe and also PbSe NC films.[11,17,20] As a second example, chemical annealing has led to unity photoconductive gains in CdSe NC films[12] and photoconductive gains greater than unity in CdTe[13] and PbS NC films.[2]

All of the methods to enhance conductivity and photoconductivity in NC films involve the exchange, removal, or decomposition of the native capping ligand on the NC surface. This modification of the NC surface can result in unpassivated states that may trap electrons and holes. In fact, it is the surface trap states, induced by chemically removing many of the ligands from CdTe NCs, that allow for photoconductive gains over 1 in CdTe NC devices.[13] When one charge carrier is trapped, the other carrier cycles through the circuit until it recombines with the trapped carrier. The enhancement of the photoconductance and photoconductive gain also depends on the nature of the contacts between the electrodes and the NC film. If the contacts are blocking, then the maximum photoconductive gain is one electron per absorbed photon, and the photocurrent is called primary. If the contact is ohmic or injecting, then the gain can be greater than unity and the photocurrent is called secondary. However, unless the mobility of one of the carriers is significantly less than the other, photoconductive gains greater than unity will not be observed regardless of the type of contact.

The trap-induced secondary photocurrents (or persistent photocurrents) can potentially last for days, if the recombination lifetime is limited by the release rate of the trap. This obviously results in slow response times.[21] Trap-induced secondary photocurrent is also not useful for solar cells because, although photocurrents may be high under applied voltage, the trapped carriers are not extracted from the device and work cannot be done by the cell. Furthermore, because the electrodes can inject charge carriers, secondary photoconductors may also have significant dark currents, which reduce their usefulness as photodetectors. A primary photoconducting system, such as a CdSe NC film contacted with gold electrodes, offers advantages over a secondary photoconducting system in that there is little to no dark current.[9,12] The observation of unity internal quantum efficiency (IQE) in such a system indicates that both electrons and holes are extracted from the film.[12] (By definition, IQE is the number of charges extracted from a device per absorbed photon. Unity IQE is equivalent to a photoconductive gain of one in a primary photoconductor.)

Butylamine-treated CdSe NC photodetectors exhibit a 50 kHz room-temperature 3-dB bandwidth,[1] a significantly faster photoresponse than the 18 Hz 3-dB bandwidth reported in a PbS

* Corresponding author. Tel: 617-253-9796; e-mail: mgb@mit.edu.
[†] Department of Chemistry.
[‡] Department of Physics.

10.1021/jp710173q CCC: $40.75
Published on Web 01/25/2008

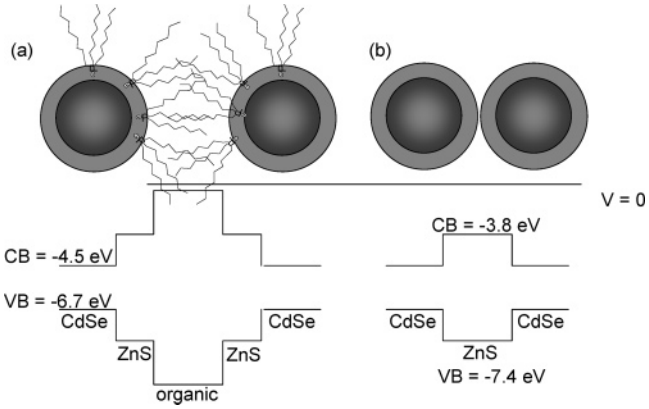

Figure 1. Schematic of a NC film and energy levels relative to vacuum for a CdSe/ZnS NC film (a) before thermal annealing and (b) after annealing to remove all of the organic ligands. The black circles are CdSe cores, and the gray rings are the ZnS shell.

NC system.[2] Despite these advantages, surface states on CdSe NCs result in an appreciable nonradiative decay rate (k_{nr}) of the exciton, except at low temperatures, thereby decreasing the room-temperature IQE. Nonradiative decay competes with radiative decay (with rate k_r) and field-assisted ionization of the exciton. Because k_{nr} decreases as the temperature decreases, photocurrents are larger in magnitude at liquid nitrogen temperature than at room temperature.[9,12] However, liquid nitrogen temperature operation is not ideal, or practical, for many optoelectronic device applications.

In this paper, we show that removing a majority of the organic ligands in a film composed of CdSe/ZnS core/shell NCs (Figure 1) results in a NC film in which (i) the magnitude of the photocurrent is larger at room temperature than low temperature and (ii) the photocurrent displays unity IQE at room temperature. The CdSe/ZnS NC films also show low dark current and a 14 kHz 3-dB bandwidth at room temperature. The experimental methods used to fabricate CdSe/ZnS NC films and remove the organic ligands are detailed, and the application of these methods to other core/shell semiconductor combinations is discussed. Our paper is divided into the following sections: In section 2, we describe sample preparation and methods for sample characterization. Section 3 summarizes our photoconductivity measurements, and section 4 discusses these results. Section 5 presents our conclusions.

2. Experimental Section

Synthesis. CdSe quantum dots are synthesized according to a previously published procedure,[3,22] as are CdSe nanorods (NR).[23−25] Methods for preparing high photoluminescence quantum yield (QY) CdSe/ZnS (core/shell) particles from $ZnEt_2$ and $(TMS)_2S$ have been reported previously[3,26,27] and are followed to grow ZnS shells on CdSe cores and CdSe NRs in this study. The method is briefly the following: the CdSe growth solution is precipitated once with methanol and centrifuged. The supernatant is discarded, and the precipitant is redissolved in 3 mL of hexane and filtered through a 0.2 μm filter. A flask with TOPO and hexaphosphonic acid (HPA) is heated to 100 °C and degassed for 1 h. The solution is cooled to 60 °C, and CdSe cores are added in hexane. Hexane is removed under vacuum (ca. 150 mTorr), and the solution is heated to 160 °C. A small amount of $CdMe_2$ (5:1 ratio Zn:Cd) is used along with $ZnEt_2$ as the cationic precursor to aid in lattice matching the ZnS shell. This is commonly termed a graded shell because the crystal structure changes gradually from CdSe to CdS to ZnS. $ZnEt_2$, $CdMe_2$, and $(TMS)_2S$ in TOP are added dropwise over the span of an hour, with the cationic and anionic precursors added in separate syringes to prevent nucleation in the syringe. Sample A is prepared in this manner.

Recently, the successive ion layer adhesion and reaction (SILAR) method has been reported as a way to achieve high QYs without the use of pyrophoric reagents.[28−30] This method also, in principle, allows layer-by-layer control of the shell material, providing greater tuning of the tunneling barrier. The reaction flask is prepared as above, with the substitution of octadecene (ODE) and octadecylamine (ODA) for TOPO and HPA. The precursors are Cd oleate, Zn oleate, and elemental sulfur in ODE. Cation and anion precursors are added alternately at 230 °C to form distinct monolayers. Using the SILAR method, a 7.5 monolayer graded shell is grown sequentially with 2 monolayers of CdS, 3.5 monolayers of $Zn_{0.5}Cd_{0.5}S$ and 2 monolayers of ZnS on the CdSe cores (Sample B). Consistent with previous literature, these nanocrystals have a QY of 59% after a single precipitation.[28] To decrease the minimum tunneling distance, a procedure for thin shell (2−4 monolayers) SILAR particles has also been investigated. For these particles, the use of CdS buffer layers to reduce the lattice strain is limited by the desired shell thickness. A CdSe/ZnS particle with a two-monolayer shell (Sample C) has been grown with one monolayer $Zn_{0.5}Cd_{0.5}S$ and one monolayer of ZnS. A CdSe/ZnS particle with a shell of four monolayers (Sample D) has been grown with 1 monolayer CdS, 1 monolayer ZnCdS, and 2 monolayers of ZnS. In general, we find the SILAR method produces NCs with high QYs when the shell is grown to 4−7 layers but does not achieve QYs as high as those in NCs overcoated with $ZnEt_2$ and $(TMS)_2S$ when the shell is only 2−3 layers.

Sample Preparation. Both CdSe and CdSe/ZnS NCs are precipitated from growth solution following previous methods for making optically clear close-packed films.[9,12,31−37] First, butanol is added to an aliquot of growth solution and then methanol is added dropwise until the solution becomes cloudy. The sample is centrifuged and the supernatant discarded. The precipitate is dissolved in a minimal amount of hexane, filtered through a 0.2 μm syringe filter, and precipitated from solution a second time. The CdSe precipitate is dissolved in hexane, filtered through a 0.1 μm syringe filter, and precipitated from solution with methanol a third time after which it is dissolved in a 9:1 hexane to octane mixture and filtered through a 0.02 μm syringe filter. For the CdSe/ZnS NC sample, the precipitation is repeated twice and the final precipitate is dissolved in a 9:1 hexane to octane mixture and filtered through 0.1 and 0.02 μm syringe filters. Two precipitations are sufficient to form optically clear films of core/shell NCs. Further processing removes too many ligands and the particles are no longer soluble.

The processed NC solutions are drop-cast onto the measurement device, which consists of 200 × 800 × 0.1 μm^3 gold electrodes lithographically patterned onto a quartz substrate. The electrodes are spaced by 2 μm. The quartz substrate is attached to a 28 pin chip carrier with silver epoxy, and contacts are made from the electrodes to the chip carrier with a gold wire bonder. The NC films are between 100 and 200 nm thick. When films are drop-cast onto an uneven surface, such as the electrodes on the quartz substrate, the film thickness can vary across the device.

Postdeposition ligand exchange with butylamine and sodium hydroxide is accomplished by soaking the CdSe NC film in a 0.1 M solution of the selected ligand in acetonitrile for 10 min. The film is rinsed with acetonitrile and dried at 70 °C for 1 h.[12]

For the thermal annealing studies, NC films are deposited in air and are heated in a vacuum oven for 30 min at a pressure of 12 mTorr.

To exchange the ligand shell of CdSe/ZnS NCs with butylamine and then deposit a film, we precipitated CdSe/ZnS NCs from solution two times and, instead of dispersing them in the hexane/octane solution, the NC powder is dispersed in 1 mL of butylamine. The sample is stirred in butylamine overnight and then precipitated with methanol, dispersed in a 9:1 hexane: octane mixture, and drop-cast onto the device. To remove the butylamine ligands after deposition, this film is soaked in methanol for 5 min and heated at 100 °C for 1 h.

Characterization Measurements. Samples are loaded into a Janis VPF-100 cryostat and measurements are performed under vacuum. A Keithley 6517 electrometer is used to measure current and source the voltage, and the samples are photoexcited with the 514 nm line of an Ar^+ laser. Unless otherwise stated, the excitation intensity is 32 mW/cm^2. The bandwidth is measured using an ISOMET 1206C acousto-optic modulator to vary the frequency of laser excitation, while the photocurrent is amplified using a Keithley 428 current amplifier and measured with a Stanford Research Systems SR830 DSP lock-in amplifier.

A JEOL 200 CX electron microscope is used to image the NCs. Samples for TEM are prepared by drop-casting a NC solution in 9:1 hexane:octane onto a carbon TEM grid. This solution is ∼200 times more dilute than the solution used to make films for conductance measurements. The average diameter of the CdSe/ZnS NCs used in this study is found by averaging the diameter measured using TEM of 50 NCs for each sample. The thickness of the ZnS shell is obtained by subtracting the diameter of the CdSe core, determined from the optical absorbance spectrum, from the diameter of the CdSe/ZnS particles determined from TEM.

Thermogravimetric analysis (TGA) measurements are performed on a Seiko Dual TG/DTA 320 Thermogravimetric/Differential Thermal Analyzer. CdSe/ZnS NCs are deposited onto a platinum sample boat from a 9:1 solution of hexane: octane. The sample boat is filled with the NC solution and, when the solvent evaporates, ∼2 mg of NCs is left behind (the boat is weighed before and after film deposition). The change in mass is monitored as the temperature is ramped from 50 to 600 °C at a rate of 10 °C per min. The mass is recorded every 0.5 s.

For FTIR studies, a film of CdSe/ZnS NCs is deposited onto a BaF_2 IR window. The FTIR spectrum from 4000 to 1000 cm^{-1} is taken with a Perkin-Elmer System 2000 FTIR before and after heating in the vacuum oven at 300 °C. The absorbance spectrum of the film on the IR window, and also of other films deposited on glass slides, is measured from 300 to 1000 nm using a Cary 5000 NIR/UV−visible Spectrometer.

To find the interparticle spacing in CdSe/ZnS NC films, samples are drop-cast on a clean piece of silicon and measured using glancing incidence small-angle X-ray scattering (GISAXS). The samples are mounted on a PANalytical X'PERT PRO multipurpose diffractometer, and the diffraction signal is monitored as theta and two-theta are swept in unison from 0.5 to 5° with data collected every 0.167°. The accelerating voltage on the copper anode is 45 kV, and the current is 40 mA. The interparticle spacing is found by taking the Fourier transform of the GISAXS signal to find the pair distribution function via a method described in previous publications.[12,37]

The quantum yield (QY) of each CdSe/ZnS and CdSe NC sample is found by taking the ratio of the sample's fluorescence to that of a Rhodamine 610 reference dye of the same absorbance at 495 nm. The NCs are excited with a 150 W ozone free xenon arc lamp through a monochromator and the fluorescence detected by a photomultiplier tube using a Horiba Jobin-Yvon Fluoromax-3 spectrometer. The QY reported for the samples in this paper is the solution QY after two precipitations. These QYs are lower than many of the NC QYs reported in the literature. We believe it is important to give the QY of the NC solution from which the films are deposited, rather than the QY of the growth solution, as the QY decreases with precipitations because of the removal of excess ligands from the solution and from the surface of the NCs.

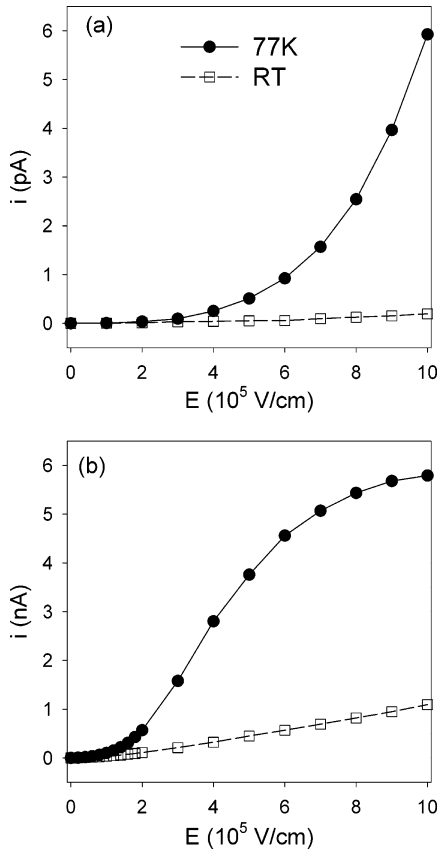

Figure 2. Photocurrent vs electric field curves for a CdSe NC film (a) before chemical treatment and (b) after treatment with 0.1 M butylamine in acetonitrile. The closed circles designate photocurrent measured at 77 K, while the open squares represent photocurrent measured at room temperature. Both the solid and dotted lines serve as guides for the eye.

3. Results

In this section, electrical measurements of CdSe/ZnS NC films before and after ligand removal are presented. A few electrical measurements on chemically treated CdSe NC films are also provided in order to compare and contrast the two systems. For the CdSe/ZnS NC films, results are given for samples having ZnS shells of differing quality and thickness, as well as for samples, for which the organic ligand is removed with different methods. Characterization of the CdSe/ZnS NC films after ligand removal is presented, as well as preliminary measurements evaluating the potential of CdSe/ZnS NC films as a material in photodetectors. Finally, photoconductivity measurements in CdSe/ZnS nanorod (NR) films are shown, to demonstrate how the methods used to build the CdSe/ZnS NC solids can be applied to other core/shell systems.

Figures 2 and 3 display photocurrent versus electric field measurements for chemically treated CdSe NC films. Photocurrent versus electric field curves for CdSe NC films with

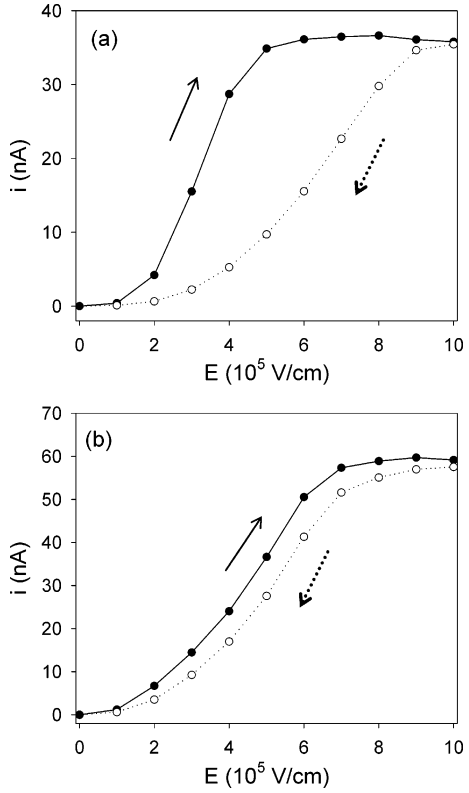

Figure 3. Photocurrent vs electric field measured at 77 K for CdSe NC films treated with 0.1 M sodium hydroxide in acetonitrile. The photocurrent measured for the sample in a displays greater hysteresis than the photocurrent of the sample in b. The closed circles represent current as the field is swept from 0 V/cm to 10×10^5 V/cm while the open circles represent the current as the field is swept from 10×10^5 V/cm back to 0 V/cm. The solid and dotted lines serve as guides for the eye. The photocurrent is steady-state and does not decay during the time scale of these experiments. Hysteresis is observed only with the sweeping of the electric field.

trioctylphosphine oxide as the capping ligand are shown in Figure 2a and for the same films after chemical treatment with 0.1 M butylamine in acetonitrile in Figure 2b. The electric field is swept from 0 to 10×10^5 V/cm in both graphs. Although the magnitude of the photocurrent is 3 orders of magnitude greater after chemical treatment, in both plots the photocurrent measured at room temperature (open squares) is lower in magnitude than the photocurrent measured at 77 K (closed circles).

Photocurrent versus electric field plots of CdSe NC films treated with 0.1 M sodium hydroxide in acetonitrile are displayed in Figure 3. In Figure 3a and b, the electric field is swept from 0 to 10×10^5 V/cm and from 10×10^5 V/cm back to 0 V/cm. Although the films are made from the same size CdSe NCs, and chemically treated in the same manner, there is significant variation between Figure 3a and b in the amount of hysteresis observed in the photocurrent between forward and reverse sweeps of the electric field reflecting strong sensitivity to details of the processing steps and small differences in the chemical environments around the NCs.

The electrical characterization of the CdSe/ZnS NC film (Sample A) giving the highest room-temperature photocurrent after removal of the organic ligands is displayed in Figures 4−7, and the physical characterization of this film is provided in Figures 8 and 9. Sample A has a 0.26 ± 0.2 nm ZnS shell and a QY of 25% in solution. The variation of the photocurrent with electric field is shown in Figure 4 at room temperature (RT) and 77 K, sweeping the field from 0 to 10×10^5 V/cm. The

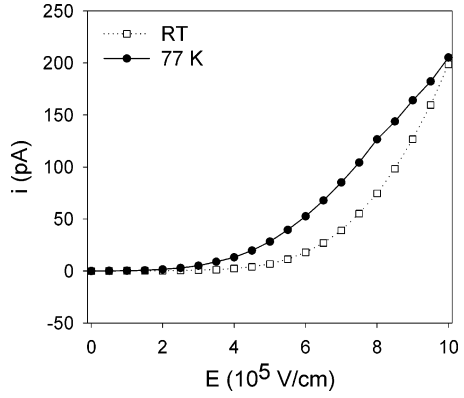

Figure 4. Photocurrent vs electric field for a CdSe/ZnS NC film. The closed circles represent photocurrent measured at 77 K while the open squares designate photocurrent measured at room temperature (RT). The photocurrent is not scaled, and the lines serve as guides for the eyes.

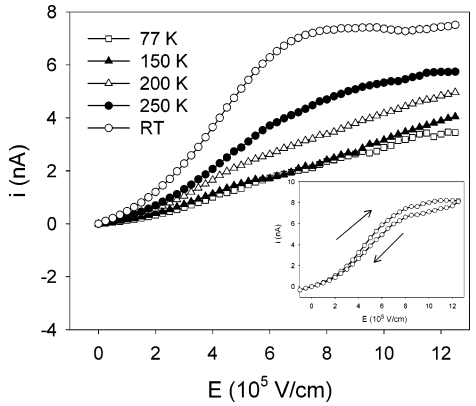

Figure 5. Photocurrent vs electric field for a CdSe/ZnS NC film annealed at 300 °C measured at various temperatures. The inset is the room-temperature photocurrent swept from 0 to 12×10^5 V/cm and then from 12×10^5 V/cm back to 0 V/cm.

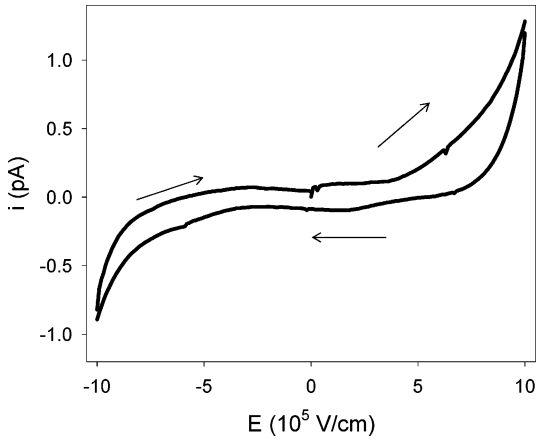

Figure 6. Dark current for a CdSe/ZnS NC film annealed at 300 °C and measured at room temperature. The electric field is swept from 0 to 10×10^5 V/cm, from 10×10^5 V/cm to -10×10^5 V/cm, and finally from -10×10^5 V/cm back to 0 V/cm.

magnitude of the photocurrent at RT (open squares) is close to that of the photocurrent measured at 77 K (closed circles).

In Figure 5, the photocurrent versus electric field is displayed for Sample A after heating in a vacuum oven at 300 °C. The photocurrent is measured at 77 K (open squares), 150 K (closed triangles), 200 K (open triangles), 250 K (closed circles), and at room temperature (open circles), sweeping the electric field from 0 to 12.5×10^5 V/cm. The photocurrent measured at room

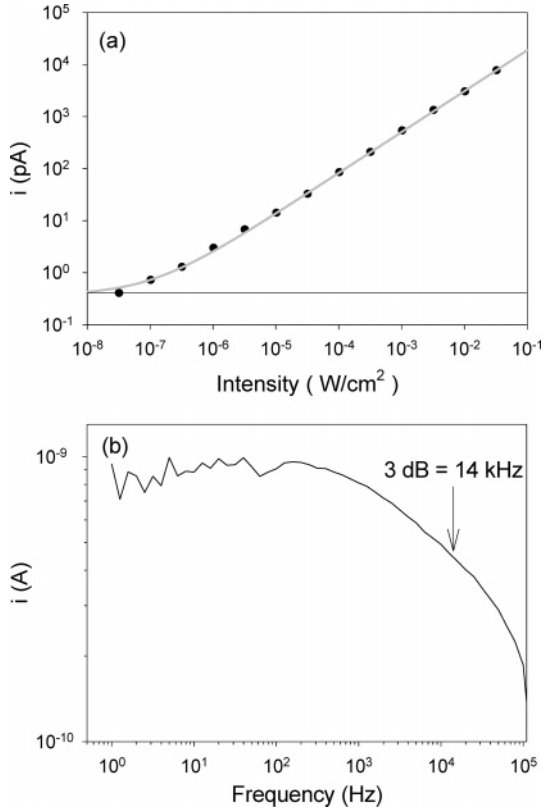

Figure 7. (a) Photocurrent as a function of intensity of 514 nm excitation light and measured at 9×10^5 V/cm (closed circles). The solid horizontal line represents the 0.37 pA of dark current in the sample at 9×10^5 V/cm. The gray line is a power law fit to the data with a y intercept of 0.37 pA and exponent of 0.8. (b) Frequency response of the photocurrent at 9×10^5 V/cm and 2.7 mW/cm^2. The 3-dB bandwidth of the device is 14 kHz.

temperature is the largest in magnitude and saturates with applied field at about 7×10^5 V/cm and 7.4 nA. The magnitude of the photocurrent decreases as the temperature is lowered, and the photocurrent no longer saturates at lower temperatures. The inset of Figure 5 shows the photocurrent at room temperature as the field is swept from 0 to 12.5×10^5 V/cm and back to 0 V/cm. There is little hysteresis.

Figure 6 shows the dark current measured at room temperature for Sample A. Some additional characteristics of Sample A are provided in Figure 7. Figure 7a gives the photoresponse of the device as a function of excitation light intensity. The photorespnse is fit with a power law having an exponent of 0.8. The dark current at 9×10^5 V/cm is 0.37 pA, and photocurrent can be detected above the dark current at 0.1 μW/cm^2 of 514 nm light. The frequency response of the device is displayed in Figure 7b, showing a 3-dB roll off at 14 kHz. This is consistent with the slowest decay of the photocurrent measured on an oscilloscope after removing the steady-state photoexcitation.

Figures 8 and 9 show data taken in order to characterize the physical and optical properties of Sample A. Figure 8a displays TGA results. The black line is the change in mass of the sample as a function of temperature. The gray line is the derivative of the black line, shown to emphasize the temperatures at which changes in mass occur. By 300 °C, 0.6 mg of the sample is lost, which is ~30% of the total sample mass. For Sample A consisting of CdSe/ZnS NCs capped with octadecylamine, a loss of all of the organic ligand should result in a ~30% decrease in sample mass,[38] consistent with the TGA measurement. The physical identity of the 0.2 mg of material lost around 410 °C

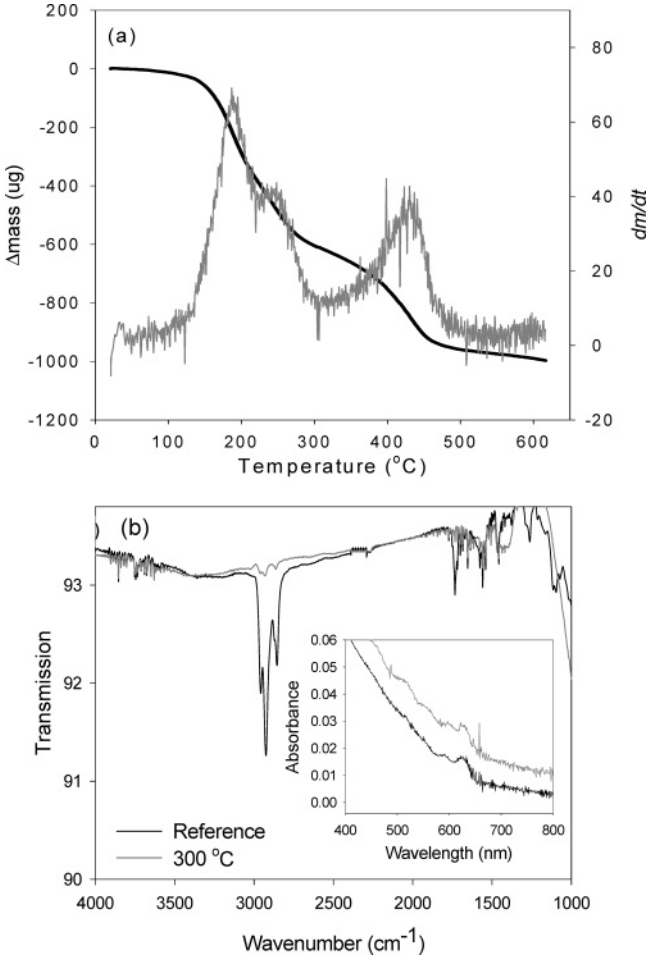

Figure 8. (a) Thermal gravimetric analysis data for a 2 mg sample of ZnS/CdS/CdSe NCs. The solid black line represents the change in mass of the NC sample as a function of temperature. The gray line is the derivative of the solid line to accentuate the change in mass. (b) FTIR spectra (wavenumbers) of a CdSe/ZnS NC film on a BaF_2 IR window before (black line) and after (gray line) vacuum annealing at 300 °C. The inset shows the UV−vis absorbance spectra (wavelength) of the same film in the region of the band edge before and after heating. The latter absorbance has been shifted on the vertical axis (only the plots in the inset have been shifted) to more clearly see the shape of the curve after heating, but neither spectrum has been multiplied by a scale factor.

is unknown; however, the NC films are not heated above 350 °C when annealing for transport measurements.

Figure 8b shows the FTIR spectra for a film of CdSe/ZnS NCs (Sample A) before (black line) and after (gray line) heating to 300 °C. The magnitude of the C−H stretching mode at 3000 cm^{-1} is reduced greatly after heating, indicating the loss of organic material from the film. The inset shows that the band-edge absorbance spectra of this sample does not change, indicating that there is no loss of inorganic material during the annealing process.

Figure 9a also displays the absorbance spectra for CdSe/ZnS NC films (Sample A), but for a variety of different annealing temperatures. Curve a is for the sample before heating, b−e are after heating at 200, 250, 300, and 350 °C, respectively, for 30 min. There is not much change in the position of the first absorption feature in the samples heated at 200, 250, or 300 °C, indicating that the NCs retain their structure and quantum confined optical properties, but all absorbance features are broadened upon heating to 350 °C.

GISAXS is used to monitor the interparticle spacing as a function of heating temperature, and the results are shown in

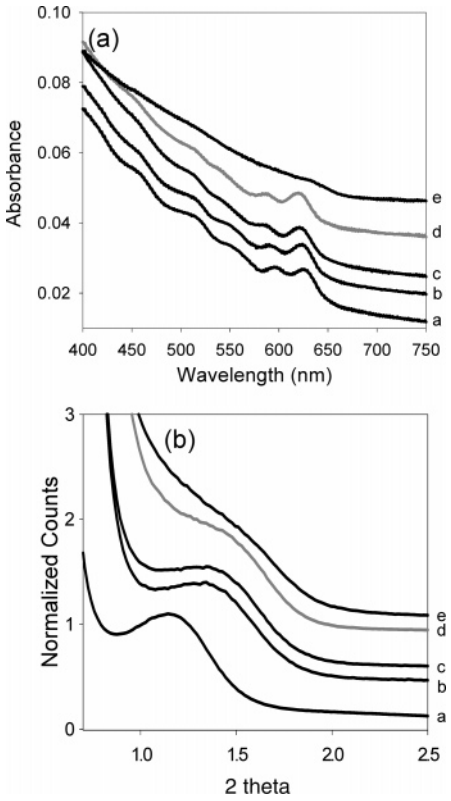

Figure 9. (a) Absorbance spectra of the CdSe/ZnS film as a function of vacuum annealing temperature. The spectra are offset along the vertical axis for clarity, but none of them have been scaled. (b) GISAXS of the CdSe/ZnS film as a function of temperature. The following correspond to the same vacuum annealing temperature in 5a and b: as-deposited (a), 200 °C (b), 250 °C (c), 300 °C (d), 350 °C (e).

Figure 9b. The labels correspond to the same heating temperatures as in Figure 9a. The NCs in Sample A have a diameter of 6.15 + 0.4 nm as measured by TEM. By subtracting the NC diameter from the spacing determined from GISAXS, the interparticle separations are calculated to be 1.25 nm before heating, and ~0.25 nm after heating to 200 °C or 250 °C. The peak in the GISAXS data, which represents the center-to-center NC spacing, is broadened significantly after heating to 300 °C and cannot be fit to extract an interparticle separation. After heating at 350 °C, the peak is completely gone. The loss of the GISAXS peak indicates that many of the NCs are touching after heating to 300 °C and that most, if not all, of the NCs touch after heating to 350 °C. These data, together with the absorbance spectra in Figure 9a, suggest that, although most of the NCs are touching after heating at 300 °C, the optical excitations are still localized because the absorbance spectrum remains intact. After heating at 350 °C, the loss of features in the absorbance spectrum indicates that the NCs have sintered into a polycrystalline bulk film and that the ZnS shell and CdSe cores are no longer distinct.

In Figure 10, conductivity measurements are presented for CdSe/ZnS NC films with ZnS shells of differing thickness and quality. Figure 10a shows the photocurrent after annealing for Sample B, which has a thick CdS/ZnS graded shell of 1.75 ± 0.17 nm and a QY of 40%. Figure 10b is after annealing Sample C, which has a thin 0.34 ± 0.1 nm shell and a QY of 4%. Last, Figure 10c gives the photocurrent versus electric field plots for a CdSe/ZnS NC film, in which the organic ligands are removed with a chemical ligand exchange followed by mild heating, as opposed to a high-temperature vacuum annealing. This CdSe/ZnS NC film (Sample D) has a 0.57 ± 0.12 nm shell. For Sample D, the TOPO capping ligand has been largely exchanged in solution with butylamine, after which the NCs are deposited on the device. The device is subsequently soaked in methanol and heated at 100 °C to remove organic ligands. The photocurrent does not saturate in any of the samples measured in Figure 10, unlike that of Sample A (Figure 5), indicating an IQE that is less than unity. All of the CdSe/ZnS NC films display room-temperature photocurrent that is larger in magnitude than the low-temperature photocurrent at 10×10^5 V/cm. The absolute magnitude of the photocurrent cannot be directly compared from sample to sample because the absorption of each device is different. However, the electric field dependence of the photocurrent can be directly compared because the length and width of the electrodes are the same for all samples.

Photocurrent results for a CdSe/ZnS nanorod film heated to 300 °C are shown in Figure 11. The photocurrent measured at room temperature (open squares) is larger in magnitude than the photocurrent measured at 77 K (closed circles), and it displays near saturation with electric field at a current close to that expected for unity IQE.

4. Discussion

In this section, a brief review of the theory of primary photoconductivity in NC films is presented in order to elucidate how the surface of the NC can cause the photocurrent to be smaller at room temperature than at low temperature, and how this temperature dependence is reversed when the CdSe NCs are overcoated with ZnS. For an in-depth analysis of primary photoconductivity in CdSe NC films, we refer to Jarosz, et al.[12] The advantages of the CdSe/ZnS NC film over chemically treated CdSe NC films are discussed, as well as the benefits of a primary photodetector such as CdSe/ZnS NCs between gold electrodes. Finally, some of the key parameters that must be considered when constructing core/shell NC films are discussed.

Primary Photoconductivity in NC Films. Equation 1 is an expression for photoconductivity in a bulk semiconductor,[21] modified to include a field-dependent exciton separation efficiency, $\eta(E)$, characteristic of CdSe semiconductor NCs.[12]

$$i = e \cdot I \cdot A \cdot \eta(E) \cdot G \tag{1}$$

In eq 1, e is the charge of an electron, I is the flux of the excitation light in units of photons per second, A is the absorption of the film in units of excitons per photon, $\eta(E)$ is the exciton separation efficiency, and G is the photoconductive gain. Substituting expressions for $\eta(E)$ and G in eq 1, we have

$$i = e \cdot I \cdot A \cdot \frac{k_E(E)}{k_E(E) + k_r + k_{nr}} \cdot \frac{(\mu_n \tau_n + \mu_p \tau_p) \cdot E}{L} \tag{2}$$

In eq 2, $\eta(E)$ is written in terms of the rates that determine its value:[9] $k_E(E)$ is the electric-field-dependent rate of exciton ionization; k_r is the radiative relaxation rate; and k_{nr} is the nonradiative relaxation rate. Faster radiative or nonradiative rates give rise to smaller exciton separation probabilities for a given field. In eq 2 G, the photoconductive gain, is expressed in terms of microscopic quantities: μ_n (μ_p) is the mobility of the electron (hole), τ_n (τ_p) is the recombination lifetime of the electron (hole), E is the applied electric field, and L is the distance between the two electrodes. This term can be further reduced to $G = (l_n + l_p)/(L)$ where l_n (l_p) is the distance traveled by an electron (hole) before recombination.[21] With blocking electrodes, when both the electron and hole reach the electrodes, the distances traveled by the two carriers add up to L, G becomes equal to 1, and the photocurrent saturates with applied electric field. We therefore

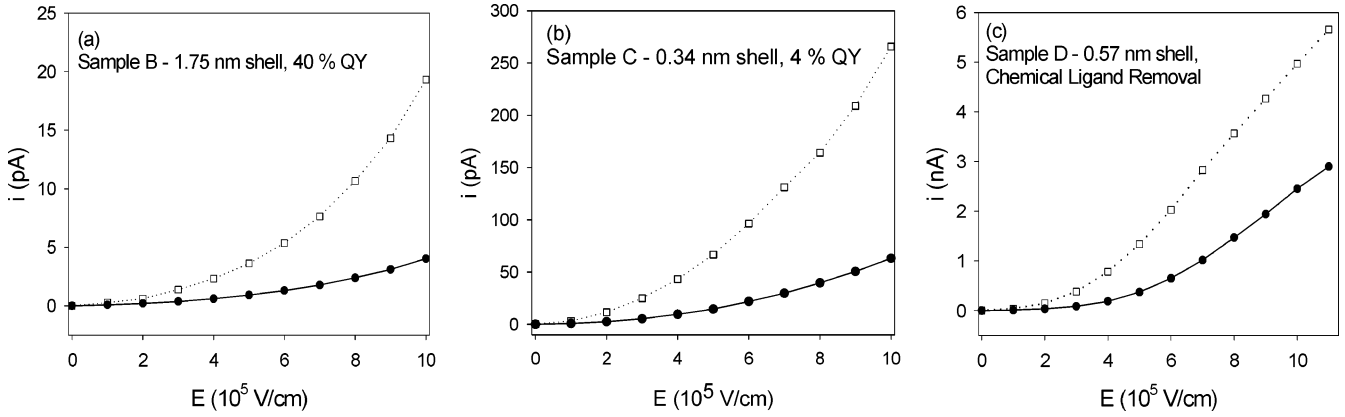

Figure 10. Photocurrent vs electric field for (a) Sample B, (b) Sample C, and (c) Sample D. The open squares represent photocurrent measured at room temperature, while the closed circles stand for photocurrent measured at 77 K. The solid and dotted lines are guides to the eye.

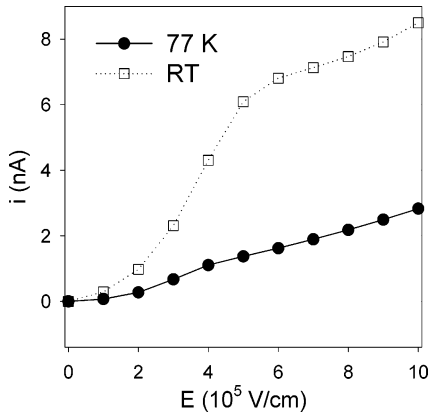

Figure 11. Photocurrent vs electric field for CdSe/ZnS nanorods heated to 300 °C. The open squares represent photocurrent measured at room temperature while the closed circles stand for photocurrent measured at 77 K. The solid and dotted lines are guides to the eye.

take the observation of saturation of photocurrent with field to indicate that all carriers are swept out of the sample.

Effect of k_{nr} on the Photoconductivity in CdSe NC Films. Equation 2 explains the observed dependence of the photocurrent on field and temperature in CdSe NC films. Both the field and temperature dependence come from the $\eta(E)$ term. The photocurrent in Figure 2a increases exponentially with field because the rate $k_E(E)$ comes from charge carrier tunneling from the NC, in which it is created, to a neighboring one. For fixed field, the photocurrent is larger at low temperature because k_{nr} is smaller at low temperature.[9,12,31] After treatment with butylamine to decrease interparticle spacing, the field dependence displays saturation of photocurrent with electric field, indicating that every charge carrier is extracted at the electrodes (Figure 2b).[12,31] However, saturation is only observed at 77 K, suggesting that at room temperature a larger electric field must be applied to separate the exciton before it recombines nonradiatively. Even after increasing the photocurrent by a factor of 1000 by decreasing interparticle spacing, the magnitude of the photocurrent is still limited by k_{nr}.

Having photocurrent that increases in magnitude as the temperature decreases is unusual for semiconductors. Usually, the current decreases with decreasing temperature because charge carriers do not have enough thermal energy to escape from trap states to the conduction band. Trap states are active in the CdSe NC film; however, the temperature dependence of k_{nr} still dominates the magnitude of the photocurrent. The effect of trap states can be observed in the hysteresis of the photocurrent upon sweeping the electric field. Figure 3a shows that significant hysteresis can be observed in photocurrent measured at 77 K after chemical treatment with sodium hydroxide. The amount of hysteresis varies from sample to sample (Figure 3a and b) even if samples undergo the same chemical treatment. This most likely occurs because each NC is capped with a different number of ligands, which are removed and replaced during ligand exchange. If more ligands are removed than are replaced, then unpassivated Cd or Se atoms remain exposed on the surface and become trap sites.

Enhancing Room-Temperature Photoconductivity with CdSe/ZnS NC Films. *(i) CdSe/ZnS NC Films with Organic Ligands.* Although chemical treatments do an excellent job of enhancing the magnitude of the photocurrent, it would be preferable if unity IQE of the photocurrent occurred at lower fields at room temperature, rather than 77 K. To extract all of the charge carriers from a CdSe NC device, one must either either run the device at much higher fields to overcome k_{nr} or cool and operate the device in a temperature range where there are many active trapping states. In this study, CdSe NCs are passivated with a shell of ZnS to reduce k_{nr}. ZnS has a larger band gap than CdSe (Figure 1) and has been shown to significantly increase the quantum yield (QY) of NCs because it electrically confines the electron and hole wavefunctions, reducing their overlap with the surface.[26,27] In Figure 4, the photocurrents measured at room temperature and 77 K in a film of CdSe/ZnS NCs are of the same order of magnitude. This implies that the dependence of the photocurrent on k_{nr} is reduced. However, the photocurrent in this film does not display saturation of photocurrent with voltage. Although adding the inorganic shell reduces k_{nr}, it also increases the interparticle spacing, reducing $k_E(E)$ and making it more difficult for a charge to tunnel to a neighboring NC. This result confirms previous measurements in which CdSe/ZnS NC films did not display large photocurrents.[9]

(ii) CdSe/ZnS NC Films after Removal of the Organic Ligands. By removing most of the organic ligands, the interparticle separation can be reduced significantly. In fact, the new separation should be close to just twice the thickness of the ZnS shell capping the CdSe NCs. As demonstrated in Figures 8 and 9, heating the CdSe/ZnS NC film to 300 °C results in a film in which the majority of the ZnS shells in the film are touching, yet the electronic wave functions of each NC remain confined. The room-temperature photocurrent in Figure 5 displays saturation with applied field at a magnitude of photocurrent, which indicates extraction of an electron for every absorbed photon. The current at which saturation should occur can be calculated using eq 1.[12,31] The absorption, A, is set equal

to 5.4%. This value is determined from line d of Figure 9a, the absorbance of a CdSe/ZnS NC film drop-cast on a glass slide from the same solution used to make Sample A. $\eta(E)$ is set equal to 1, G is set equal to one, and I is set equal to the photon flux on the active area of the sample (determined from fitting the profile of the excitation beam). Using these values, we found that the calculated photocurrent is 11.8 nA, close to the 7.4 nA found experimentally in Figure 5. Two other devices deposited from this solution exhibited photocurrent saturation at 14 and 3.5 nA, consistent with variations in sample thickness. Films drop-cast onto the measurement device are not of a uniform thickness because the gold electrodes and wires cause the film to dry unevenly.

The photocurrent in Figure 5 decreases with decreasing temperature, indicating that k_{nr} is no longer the dominating factor. The photocurrent is smaller at lower temperatures because more carriers are trapped in unpassivated surface states created by the removal of the organic ligands. These CdSe/ZnS NC films show promise as a material for device applications because all electrons and holes are extracted at room temperature.

Mobility and Transit Time of CdSe/ZnS NC Films. Figure 7b displays the 14 kHz 3-dB frequency bandwidth of this device at 9×10^5 V/cm, the electric field at which the photocurrent saturates. Because the 3-dB frequency bandwidth is the inverse of the decay time, it can be used to approximate the transit time of the minority carrier. Using this value, along with the applied field and distance between the electrons (2×10^{-4} cm), the average carrier mobility in this device is calculated to be 3×10^{-6} cm^2/Vs. This mobility is used to determine that the average carrier density, η, is 2×10^{15} cm^{-3}. Given the sample volume and estimated number of NCs in the device, this carrier density translates to about one electron per 1000 NCs at a field of 9×10^5 V/cm.

Effect of the Shell on Conduction. Figure 10a demonstrates that despite a significant reduction in k_{nr} in Sample B (40% QY), the inorganic shell can be too thick to get unity IQE. The quality of the inorganic shell is also important. Figure 10b shows the photocurrent for Sample C, which has a 0.68 nm interparticle spacing (close to Sample A) but a QY of only 4% as compared to the 25% QY of Sample A. Although the room-temperature photocurrent is larger in magnitude than the photocurrent measured at 77 K, the photocurrent does not show saturation with applied field. This indicates that although k_{nr} does not hinder exciton separation, the mobility of the carriers in the film is low. This is most likely the result of trap sites that are present on the NC surface with a patchy or uneven ZnS shell, common causes for a low QY.

Heat is not the only treatment that can be used to remove the organic ligands. Figure 10c shows the photocurrent results for a film deposited from CdSe/ZnS capped with butylamine (Sample D). After removal of the butylamine ligands with a methanol treatment, the photocurrent is linear with electric field at high voltage. This indicates that every exciton is separated but one or both carriers are not extracted at the electrodes.[12] A linear response is consistent with transport of free charge carriers having lifetimes shorter than the transit time. When the carrier lifetimes approach the transit time, saturation occurs. The photocurrent does not saturate because Sample D has a thicker shell ($d = 1.14$ nm) than Sample A, decreasing the free carrier mobility. When the butylamine cap exchange is performed on Sample A, a blue shift is observed in the absorbance spectrum. This indicates that the butylamine is etching the surface of the NC. For samples with a very thin shell, this can have a significant effect on the optical properties. However, for materials in which the alloying temperature of the core and shell is lower than the temperature at which ligands are removed, cap exchange into a ligand with a lower boiling point could be used as an alternative method to create a core/shell NC film.

5. Conclusions

This paper demonstrates that it is possible to reduce the effect of nonradiative recombination on the photocurrent in close-packed films of NCs and to achieve unity IQE of the photocurrent at room temperature by overcoating NC cores with a higher band gap inorganic material and removing a majority of the organic ligands. Besides achieving high room-temperature photocurrents, this results in a change in the photoconductive mechanism from one limited by the carrier generation rate to one dominated by carrier mobility. Reducing the influence of surface states on the photoconductivity in NC films is an important step toward the potential use of these films in room-temperature photodetectors.

A number of core/shell materials can potentially be combined to create photoconductive NC solids. A first step toward creating variations of core/shell NC solids is given in this paper with the photoconductivity measurements of a CdSe/ZnS nanorod film. To achieve high conductivity in a core/shell NC film a thin, high-quality shell must be grown on the NC core. This can prove to be the most challenging step because the lattice mismatch between different semiconductors can result in core/shell NCs with low QYs. Provided a suitable shell can be grown, and the organic ligands removed, NC solids can be assembled for many different applications.

Acknowledgment. This work was funded in part by the NSF MRSEC program (DMR 0213282) at MIT, and we made use of its shared user facilities. It was also funded by the NSEC program of the National Science Foundation Award No. DMR-0117795 and the U.S. Army through the Institute for Soldier Nanotechnologies, under Contract No. DAAD-19-02-0002. We also thank Dr. Scott A. Speakman for his assistance in with GISAXS measurements and Dr. Tim McClure for help with TGA measurements.

References and Notes

(1) Oertel, D. C.; Bawendi, M. G.; Arango, A. C.; Bulovic, V. *Appl. Phys. Lett.* **2005**, *87*, 213505.
(2) Konstantatos, G.; Howard, I.; Fischer, A.; Hoogland, S.; Clifford, J.; Klem, E.; Levina, L.; Sargent, E. H. *Nature* **2006**, *442*, 180.
(3) Snee, P. T.; Chan, Y.; Nocera, D. G.; Bawendi, M. G. *Adv. Mater.* **2005**, *17*, 1131.
(4) Milliron, D. J.; Gur, I.; Alivisatos, A. P. *MRS Bull.* **2005**, *30*, 41.
(5) Gur, I.; Fromer, N. A.; Alivisatos, A. P. *J. Phys. Chem. B* **2006**, *110*, 25543.
(6) Gur, I.; Fromer, N. A.; Geier, M. L.; Alivisatos, A. P. *Science* **2005**, *310*, 462.
(7) Huynh, W. U.; Dittmer, J. J.; Alivisatos, A. P. *Science* **2002**, *295*, 2425.
(8) Morgan, N. Y.; Leatherdale, C. A.; Drndic, M.; Jarosz, M. V.; Kastner, M. A.; Bawendi, M. *Phys. Rev. B* **2002**, *66*, 075331.
(9) Leatherdale, C. A.; Kagan, C. R.; Morgan, N. Y.; Empedocles, S. A.; Kastner, M. A.; Bawendi, M. G. *Phys. Rev. B* **2000**, *62*, 2669.
(10) Drndic, M.; Jarosz, M. V.; Morgan, N. Y.; Kastner, M. A.; Bawendi, M. G. *J. Appl. Phys.* **2002**, *92*, 7498.
(11) Romero, H. E.; Drndic, M. *Phys. Rev. Lett.* **2005**, *95*, 156801.
(12) Jarosz, M. V.; Porter, V. J.; Fisher, B. R.; Kastner, M. A.; Bawendi, M. G. *Phys. Rev. B* **2004**, *70*, 195327.
(13) Porter, V. J.; Mentzel, T.; Charpentier, S.; Kastner, M. A.; Bawendi, M. G. *Phys. Rev. B* **2006**, *73*, 155303.
(14) Yu, D.; Wang, C. J.; Guyot-Sionnest, P. *Science* **2003**, *300*, 1277.
(15) Wehrenberg, B. L.; Guyot-Sionnest, P. *J. Am. Chem. Soc.* **2003**, *125*, 7806.
(16) Wang, C. J.; Shim, M.; Guyot-Sionnest, P. *Appl. Phys. Lett.* **2002**, *80*, 4.

(17) Talapin, D. V.; Murray, C. B. *Science* **2005**, *310*, 86.
(18) Shim, M.; Guyot-Sionnest, P. *Nature* **2000**, *407*, 981.
(19) Shim, M.; Wang, C. J.; Guyot-Sionnest, P. *J. Phys. Chem. B* **2001**, *105*, 2369.
(20) Yu, D.; Wang, C. J.; Wehrenberg, B. L.; Guyot-Sionnest, P. *Phys. Rev. Lett.* **2004**, *92*, 216802.
(21) Bube, R. H. *Photoconductivity of Solids*; Wiley: New York, 1960.
(22) Stott, N. E.; Bawendi, M. G. In *Chemistry*; Massachusetts Institute of Technology: Cambridge, MA, 2002.
(23) Peng, X.; Manna, L.; Yang, W.; Wickham, J.; Scher, E.; Kadavanich, A.; Alivisatos, A. P. *Nature* **2000**, *404*, 59.
(24) Peng, A.; Peng, X. G. *J. Am. Chem. Soc.* **2001**, *124*, 3343.
(25) Halpert, J. E.; Porter, V. J.; Zimmer, J. P.; Bawendi, M. G. *J. Am. Chem. Soc.* **2006**, *128*, 12590.
(26) Hines, M. A.; Guyot-Sionnest, P. *J. Phys. Chem.* **1996**, *100*, 468.
(27) Dabbousi, B. O.; RodriguezViejo, J.; Mikulec, F. V.; Heine, J. R.; Mattoussi, H.; Ober, R.; Jensen, K. F.; Bawendi, M. G. *J. Phys. Chem. B* **1997**, *101*, 9463.
(28) Xie, R. G.; Kolb, U.; Li, J. X.; Basche, T.; Mews, A. *J. Am. Chem. Soc.* **2005**, *127*, 7480.
(29) Li, J. J.; Wang, Y. A.; Guo, W. Z.; Keay, J. C.; Mishima, T. D.; Johnson, M. B.; Peng, X. G. *J. Am. Chem. Soc.* **2003**, *125*, 12567.
(30) Aharoni, A.; Mokari, T.; Popov, I.; Banin, U. *J. Am. Chem. Soc.* **2006**, *128*, 257.
(31) Jarosz, M. V. In *Department of Chemistry*; Massachusetts Institute of Technology: Cambridge, MA, 2004.
(32) Kagan, C. In *Materials Science and Engineering*; Massachusetts Institute of Technology: Cambridge, MA, 1996.
(33) Jarosz, M. V.; Stott, N. E.; Drndic, M.; Morgan, N. Y.; Kastner, M. A.; Bawendi, M. G. *J. Phys. Chem. B* **2003**, *107*, 12585.
(34) Kagan, C. R.; Murray, C. B.; Nirmal, M.; Bawendi, M. G. *Phys. Rev. Lett.* **1996**, *76*, 3043.
(35) Murray, C. B.; Norris, D. J.; Bawendi, M. G. *J. Am. Chem. Soc.* **1993**, *115*, 87065.
(36) Murray, C. B.; Kagan, C. R.; Bawendi, M. G. *Science* **1995**, *270*, 1335.
(37) Murray, C. B.; Kagan, C. R.; Bawendi, M. G. *Annu. Rev. Mater. Sci.* **2000**, *30*, 545.
(38) To calculate the total mass of ligands on this NC, it is assumed that there is one octadecylamine molecule per surface Zn atom. The mass of the organic ligands is divided by the total mass of the graded core/shell NC, calculated by taking into account the amount of Zn, Cd, S, and Se at each layer in the NC.